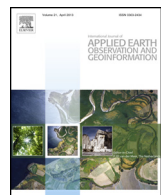




Contents lists available at ScienceDirect

International Journal of Applied Earth Observation and Geoinformation

journal homepage: www.elsevier.com/locate/jag



Individual tree crown delineation using localized contour tree method and airborne LiDAR data in coniferous forests



Bin Wu^{a,b}, Bailang Yu^{a,b,*}, Qiusheng Wu^c, Yan Huang^{a,b}, Zuqi Chen^{a,b}, Jianping Wu^{a,b}

^a Key Laboratory of Geographic Information Science, Ministry of Education, East China Normal University, Shanghai 200241, China

^b School of Geographic Sciences, East China Normal University, Shanghai 200241, China

^c Department of Geography, Binghamton University, State University of New York, Binghamton, NY 13902, USA

ARTICLE INFO

Article history:

Received 15 February 2016

Received in revised form 30 May 2016

Accepted 2 June 2016

Keywords:

Individual tree crown
Segmentation
Contour tree
Graph theory
Hierarchical structure
LiDAR

ABSTRACT

Individual tree crown delineation is of great importance for forest inventory and management. The increasing availability of high-resolution airborne light detection and ranging (LiDAR) data makes it possible to delineate the crown structure of individual trees and deduce their geometric properties with high accuracy. In this study, we developed an automated segmentation method that is able to fully utilize high-resolution LiDAR data for detecting, extracting, and characterizing individual tree crowns with a multitude of geometric and topological properties. The proposed approach captures topological structure of forest and quantifies topological relationships of tree crowns by using a graph theory-based localized contour tree method, and finally segments individual tree crowns by analogy of recognizing hills from a topographic map. This approach consists of five key technical components: (1) derivation of canopy height model from airborne LiDAR data; (2) generation of contours based on the canopy height model; (3) extraction of hierarchical structures of tree crowns using the localized contour tree method; (4) delineation of individual tree crowns by segmenting hierarchical crown structure; and (5) calculation of geometric and topological properties of individual trees. We applied our new method to the Medicine Bow National Forest in the southwest of Laramie, Wyoming and the HJ Andrews Experimental Forest in the central portion of the Cascade Range of Oregon, U.S. The results reveal that the overall accuracy of individual tree crown delineation for the two study areas achieved 94.21% and 75.07%, respectively. Our method holds great potential for segmenting individual tree crowns under various forest conditions. Furthermore, the geometric and topological attributes derived from our method provide comprehensive and essential information for forest management.

© 2016 Elsevier B.V. All rights reserved.

1. Introduction

Accurate assessment of forest resources is very important for sustainable and precise forest management (Chang et al., 2012; Kwak et al., 2007). Forest parameters, such as tree location, tree height, tree count, crown diameter and tree species, are essential for quantitative analysis of forest (Chen et al., 2006; Koch et al., 2006; Kwak et al., 2007). These individual tree-related properties are also required in various forest-related activities, such as estimation of timber stock, age structure, regrowth, ecosystem modeling and biodiversity assessments (Hu et al., 2014; Koch et al., 2006; Lichstein

et al., 2010). Obviously, the detailed information at individual tree level is the basis for forest inventory (Estornell et al., 2014; Unger et al., 2014). Traditionally, these detailed information related to forest resources have been obtained by field measurements, which are very time-consuming and labor-intensive (González-Ferreiro et al., 2013; Lee et al., 2010), and are also limited by small sample sizes and inaccessible areas (Chang et al., 2012; Lee et al., 2010). Remote sensing technologies have been proved as an effective and reliable alternative for extracting tree information and supplementing field measurements in recent decades (Strímbu and Strímbu, 2015). Among the remote sensing technology utilized, Light Detection And Ranging (LiDAR) has become one of the most efficient surveying techniques for acquiring detailed and accurate 3D data (Huang et al., 2015; Wu et al., 2016; Wu et al., 2013; Yu et al., 2010a; Yu et al., 2016). LiDAR is mainly used to record x, y and z coordinates of ground objects based on laser range measurements (Wu et al.,

* Corresponding author at: Key Laboratory of Geographic Information Science, Ministry of Education, East China Normal University, Shanghai 200241, China.

E-mail address: blyu@geo.ecnu.edu.cn (B. Yu).

2013). Among various LiDAR platforms, airborne LiDAR has been widely used for extracting tree information in forests (González-Ferreiro et al., 2013; Reitberger et al., 2008; Wagner et al., 2008; Yu et al., 2011).

Airborne LiDAR records geometric information of ground objects from the top (Wu et al., 2013), which provides essential information about the vertical and horizontal structure of forest (Strîmbu and Strîmbu, 2015). Current forest inventory studies using airborne LiDAR data can be mainly divided into two categories: (1) stand-level based analysis, in which forest stands are the basic unit of forest inventory (González-Ferreiro et al., 2013; González-Ferreiro et al., 2012; Hollaus et al., 2007; Holmgren et al., 2003; Means et al., 2000; Means et al., 1999); and (2) individual tree level based technique, in which individual trees are the basic unit of forest assessment (Chang et al., 2012; Chen et al., 2006; Ene et al., 2012; Hyppä et al., 2001; Lu et al., 2014; Yu et al., 2011).

Compared with stand-level based analysis, the approach for individual tree detection and delineation requires denser airborne LiDAR data (González-Ferreiro et al., 2013; Hyppä et al., 2001). In addition, estimation of various tree parameters through individual tree level based technique is more straightforward and labor-saving (Hyppä et al., 2008; Yu et al., 2010b). While the stand-level based approaches are based on the height and density data acquired by airborne LiDAR and do not make use of the neighborhood data of laser returns (Hyppä et al., 2012). Thus, the stand-level based approaches are usually not sufficient for forest management planning (Koch et al., 2006), which have directly led to the vigorous development of individual tree crown delineation methods (González-Ferreiro et al., 2013).

To obtain individual tree information from airborne LiDAR data, the key lies in the segmentation of individual trees. To date, numerous automated and semi-automated methods for identifying and mapping individual trees using airborne LiDAR data have been proposed in the literature. Among these studies, two types of data are mainly used: the original LiDAR point cloud and the LiDAR-derived canopy height model (CHM) (Zhao et al., 2014). The major advantage of point cloud-based individual tree detection is low information loss (Vega et al., 2014; Zhang et al., 2015; Zhao et al., 2014). Several methods have been developed for extracting individual trees from raw airborne LiDAR point clouds leading to varying degree of success. Morsdorf et al. (2004) applied the k -means clustering algorithm to segment individual trees from raw airborne LiDAR point cloud, but their accuracy largely depends on seed points extracted from the LiDAR-derived CHM. Wang et al. (2008) used a voxel structure and a morphological algorithm to retrieve tree crowns. Reitberger et al. (2009) proposed a normalized cut segmentation method that extracts individual trees from a bipartite graph in a voxel space. Lee et al. (2010) developed an adaptive region growing and clustering approach to identify individual trees directly on raw point cloud data. Li et al. (2012) developed a spacing-based algorithm which adopts a top-to-bottom region growing approach to segment trees individually in a mixed conifer forest. Vega et al. (2014) introduced the PTrees method, a multi-scale dynamic point cloud segmentation approach to extract trees from a forest from airborne LiDAR point cloud. However, these methods focusing on full exploitation of airborne LiDAR point cloud require more computing time (Zhao et al., 2014). Therefore, LiDAR-derived CHM based approaches have been developed and enhanced.

Canopy height model is a rasterized representation of forest canopy surface (Ene et al., 2012), which is computed as the difference between the digital surface model (DSM) and the digital elevation model (DEM). Many approaches utilize the LiDAR-derived CHM as the main data source to segment individual tree crowns by introducing image processing techniques and methods. Hyppä et al. (2001) derived the local maxima as the seed points from CHM

and then used region growing method to segment the tree crowns. Persson et al. (2002) identified tree location by searching for local height maxima in a smoothed CHM. Popescu et al. (2003) used the local maximum technique and a curve profile fitting algorithm to delineate tree crowns. Brandtberg et al. (2003) presented an automatic scale selection method for individual tree crowns isolation. Popescu and Wynne (2004) used a variable size image filtering method to estimate tree height by detecting individual trees. Koch et al. (2006) also applied the local maximum filter to find possible tree tops, then used a pouring algorithm to detect the crown-edges. Chen et al. (2006) detected tree tops by using a variable window size local maxima, followed by a marker-controlled watershed segmentation method to isolate trees. Pirotti (2010) used a template matching approach to extract tree height and position. Lin et al. (2011) introduced a multi-level morphological active contour algorithm to identify and delineate tree crowns in a mountainous forest. Ene et al. (2012) used a regional maxima detection method and adaptive filtering for single tree detection in a heterogeneous boreal forest. González-Ferreiro et al. (2013) also delineated tree crowns by watershed segmentation. Hu et al. (2014) used a multi-scale filtering method based on morphological techniques for individual tree crown delineation from LiDAR-derived CHM. Liu et al. (2015) proposed a Fishing Net Dragging method for individual tree crown segmentation.

Although a lot of the above-mentioned methods have reported relatively satisfactory performance, Kaartinen et al. (2012) revealed that most of the methods showed a high variability in their performance even when applied to the same dataset; the simple local maxima and watershed-based method perform well in most cases (Kaartinen et al., 2012; Strîmbu and Strîmbu, 2015). Similarly, Larsen et al. (2011) showed that forest structure has a strong influence on the performance of individual tree crown delineation algorithms. The accuracy of individual trees detection algorithm largely depends on the structural complexity of forest (González-Ferreiro et al., 2013; Vauhkonen et al., 2012). In other words, the topological relations and spatial structure among tree crowns are of vital importance for individual trees extraction (Strîmbu and Strîmbu, 2015). By addressing these shortcomings, Strîmbu and Strîmbu (2015) proposed a graph-based segmentation method for individual tree crown extraction. They used a weighted graph to construct an abstract representation of the forest structure, and identified individual trees by graph partitioning. However, the topological relations of tree crowns represented by the directed acyclic graph are still implicit in their work. Moreover, the algorithm is controlled by many parameters, which are hard to determine when the algorithm is applied to other forests. Besides, the approaches dealing with accuracy assessment of individual tree crown delineation varies in previous studies (Liu et al., 2015), which makes it difficult to compare the results due to a lack of standardized and widely applicable approach.

In this work, we aim to address the drawbacks identified above by employing the localized contour tree method (Wu et al., 2015) to extract individual tree crowns and to describe the topological relations among tree crowns. The proposed approach captures the topological structure of tree crowns and quantifies their topological relationships in a graph by using the graph theory-based localized contour tree method, and finally segments individual tree crowns by analogy of recognizing hills from a topographic map. The research objectives of this study were to (a) develop a robust tree crown delineation approach that can detect individual tree crowns with high accuracy; (b) construct an explicit and clear representation of topological relationships among tree crowns and (c) develop a simple accuracy assessment method to evaluate performance of the proposed methodology. The proposed methodology consists of five key steps: (1) derivation of canopy height model from airborne LiDAR data; (2) generation of contours based on the canopy height

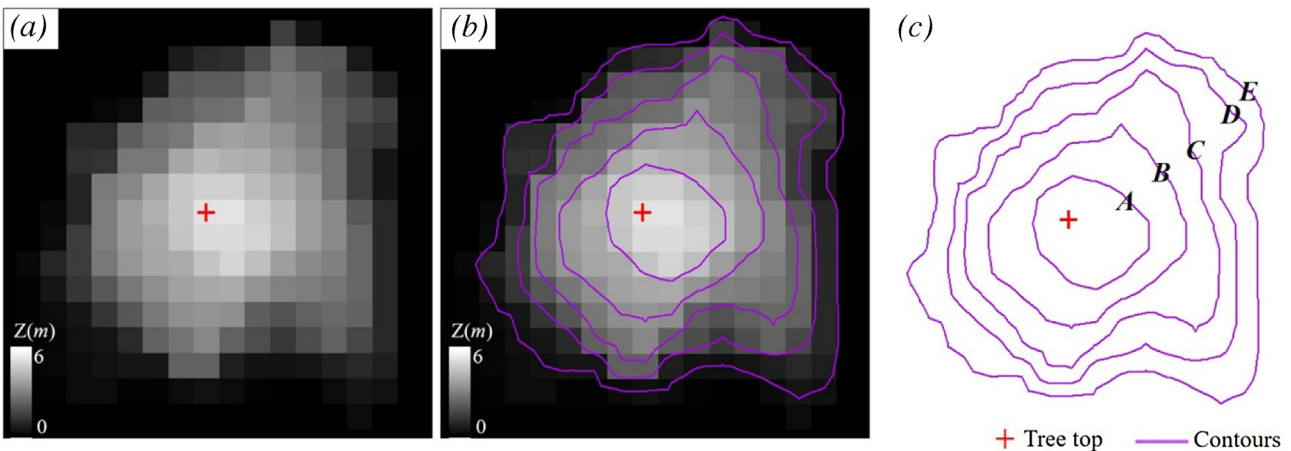


Fig. 1. An individual tree: (a) canopy height model; (b) contours generation; (c) contour representation.

model; (3) extraction of hierarchical structures of tree crowns using the localized contour tree method; (4) delineation of individual tree crowns by segmenting hierarchical crown structure; and (5) calculation of geometric and topological properties of individual trees. These five steps are explained in detail in Section 2 along with the introduction of the accuracy assessment method. In Section 3, the performance of our proposed individual tree crown delineation method was evaluated through two case studies. Section 4 provides a comparison of the results and a discussion of the parameters. Finally, the conclusions are drawn in Section 5.

2. Methodology

2.1. Outline

In our study, tree canopies are treated as a subset of surface uplifts in a rasterized CHM. In the CHM, an individual tree consists of a local maxima and a set of spatially connected grid cells of low height values, which is treated as a surface uplift. The local maxima is referred to as the tree top, and its height value is higher than or equal to that of its eight neighbors. In Fig. 1(a), a tree is represented by bright pixels surrounded by lower height pixels in the dark areas. In essence, we can treat the CHM like a topographic surface, and each individual tree is a surface uplift. While in a vector-based contour representation, an individual tree is indicated by a series of concentric closed contours with height value increasing from outer contours to inner contours (Fig. 1(b)). Since trees in a forest may vary in size and shape, structure and composition of tree canopies can be highly complex due to tree crown overlap (Fig. 2(a)). The complex crown-overlapping trees are manifested by the nested relationships of several sets of concentric closed contours (Fig. 2(b)). The boundary of an individual tree crown corresponds to the outmost closed contour in a single concentric structure. While for the composite concentric structure, the crucial procedure is to correctly identify single concentric contours from the complex concentric contours. To address this issue, the localized contour tree method (Wu et al., 2015), originally developed to delineate surface depressions, was adopted and improved to identify and resolve these complex (single or composite) concentric structures. This graph theory-based contour tree algorithm detects each single or composite concentric structure as one local contour tree. The delineation of individual tree crowns in our method is realized by segmenting the outmost contour with the valley line pass through the detected saddle point. The detailed steps are described subsequently.

2.2. Proposed method

2.2.1. Derivation of canopy height model from airborne LiDAR data

As noted earlier, the individual tree crown delineation from airborne LiDAR point cloud data is typically based on a canopy height model, which is the difference between Digital Surface Model (DSM) and Digital Elevation Model (DEM). The DSM grid was interpolated from the raw LiDAR point cloud by using the linear Triangulated Irregular Network (TIN) interpolation method. The DSM contains elevation information for all objects and ground features, including trees and other natural objects. To get absolute vegetation height from the raw LiDAR cloud points, influence of terrain must be removed. Thus, the DEM was used for normalization of the raw LiDAR point heights. In our study, the DEM was derived from ground-classified LiDAR points which had been classified using a progressive morphological filter (Zhang et al., 2003). Cell size of the grid is a key parameter in constructing the CHM (Chen et al., 2006; Strîmbu and Strîmbu, 2015). Appropriate cell size will help to avoid raster gaps and preserve sufficient details. According to Chen et al. (2006), the grid cell size (c) can be set as

$$c = \sqrt{1/n} \quad (1)$$

where n is the pulse density (returns/m²).

After careful selection of the grid cell size, data noise or errors may still exist in the CHM. Therefore, a Gaussian smoothing filter (Eq. (2)) was used to reduce data noise:

$$G(x, y) = \frac{1}{2\pi\sigma^2} e^{-\frac{(x^2+y^2)}{2\sigma^2}} \quad (2)$$

where G is a Gaussian kernel of standard deviation σ and centered at location (x, y) . The convolution filter algorithm has a smoothing effect with the standard deviation (σ) acting as a reduction factor. The smoothed CHM eliminates most of the noise and empty pixels, thus allowing easier interpretation of tree crowns. The smoothed CHM was used in subsequent analyses.

2.2.2. Generation of contours based on canopy height model

Based on the smoothed CHM, we created vector contours. When generating the contours, two important parameters need to be set: the minimum canopy height (d_0) and the vertical resolution (d). In general, contours are generated above the minimum canopy height. Considering the existence of small shrubs and some low ground objects in the smoothed CHM, these non-tree pixels can be eliminated by setting the minimum canopy height. In Strîmbu

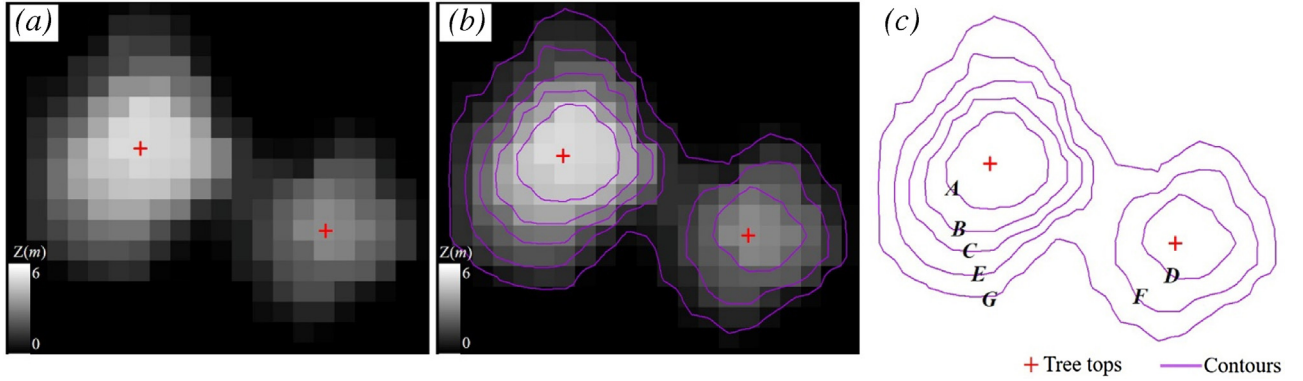


Fig. 2. Two overlapped trees: (a) canopy height model; (b) contours generation; (c) contour representation.

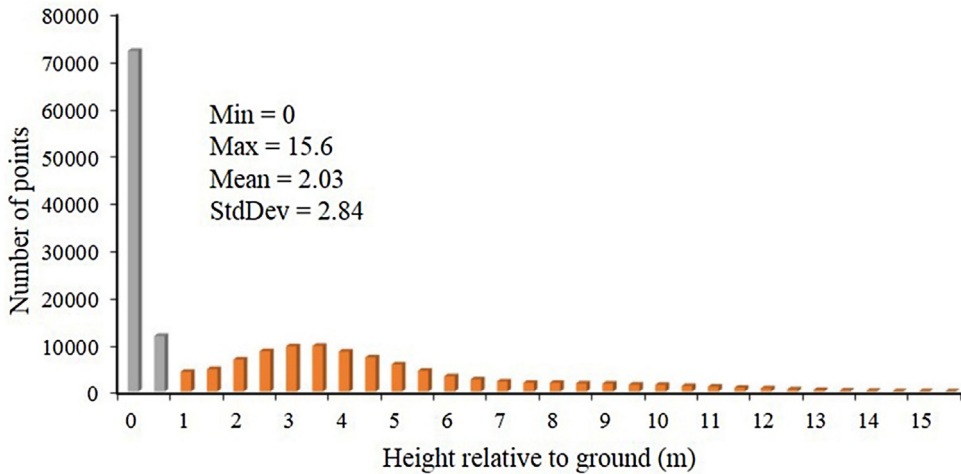


Fig. 3. LiDAR point height distribution. Points within the grey height intervals have been eliminated.

and Strîmbu (2015), the height threshold for non-tree pixels elimination was selected by analyzing the height (relative to ground) histogram of the LiDAR points. Similarly, the appropriate minimum canopy height d_0 was selected by analyzing the height histogram of non-ground points in our study. The non-ground points were extracted by removing the ground points identified in Section 2.2.1 from the original LiDAR points. As shown in Fig. 3, the mean height relative to ground is 2.03 m and the standard deviation is 2.84 m. Approximately 35.9% of the non-ground points fall within the 0–0.8 m interval. Therefore, the points within the grey height interval should not be considered, thus the minimum canopy height was set to 0.8 m. Another parameter vertical resolution d (the difference in elevation between successive contour lines) also affects the generation of contour lines. A large vertical resolution will generate few contour lines, which may lose some information of tree crowns and lead to large omission errors. On the contrary, a very small vertical resolution could dramatically increase data volume. As a rule of thumb, one can choose the vertical resolution slightly greater than the vertical accuracy of the LiDAR-derived CHM (Wu et al., 2015). More details about the selection of vertical resolution will be discussed in Section 4.2.

2.2.3. Extraction of hierarchical structures of tree crowns using localized contour tree method

In a contour map, trees are represented as closed contours surrounded by other closed contours at lower height. Topological relationships between closed contours can be represented by

a contour tree. The localized contour tree method was first proposed to identify surface depressions (Wu et al., 2015) and the authors treated the surface depression detection problem as the identification of a set of concentric contours with an increasing elevation outward, which is represented by a contour tree. A single depression is spatially independent of other depressions which can be represented by a single-branch contour tree, while a complex nested depression is represented by a multi-branch contour tree. More information about the conceptual framework of the localized contour tree method can be found in Wu et al. (2015).

In this study, we adopted and refined the localized contour tree algorithm for individual tree crown delineation. There are two types of contours on a contour map: open contours and closed contours. An open contour has a starting and an ending point that intersect map edges at different locations, while a closed contour is continuous without intersections with the map edges, forming a loop. Each contour is attributed with its contour value (elevation) and its adjacent contour. As mentioned before, the tree crowns are a subset of surface uplifts in the smoothed CHM, which are represented as closed contours that are surrounded by other closed contours at a lower elevation in the contour maps. Consequently, only closed contours with a concentric pattern are kept for subsequent analysis, while open contours are ignored. Extracting hierarchical structures of tree crowns includes two steps: (1) identify concentric contours; and (2) construct local contour trees.

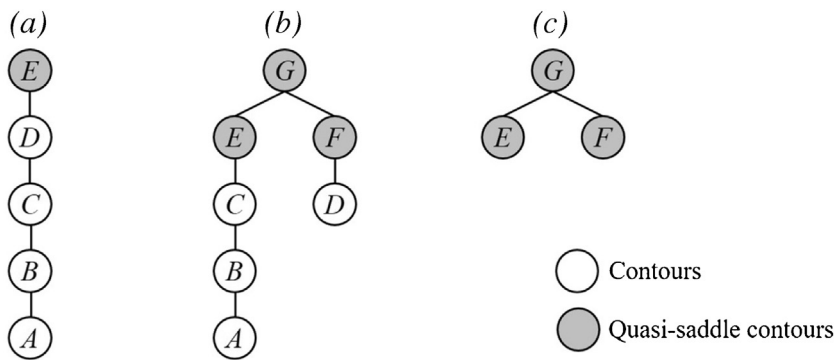


Fig. 4. Illustration of local contour tree representation for trees: (a) a single-branch contour tree representation of the individual tree shown in Fig. 1; (b) a multi-branch contour tree representation of the overlapped trees shown in Fig. 2; (c) a simplified contour tree representation of the overlapped tree shown in Fig. 2.

2.2.3.1. Identify concentric contours. To identify concentric contours, one key step is to identify 'seed contours', which are defined as the innermost closed contours that do not enclose any other contours. In the contour map derived from the smoothed CHM, tree crowns serve as a set of uplifts, so the seed contours represent tree top areas which have a higher elevation than the contours located in the outward. The region surrounded by the seed contour is typically small, so the center of the region is regarded as the tree top in our study. Fig. 1(c) and Fig. 2 (c) illustrate the contour representation of an individual tree shown in Fig. 1(a) and two trees with crown overlap shown in Fig. 2(a), respectively. In Fig. 1(c), contour **A** is a seed contour, whereas contours **B**, **C**, **D** and **E** are not. In Fig. 2(c), contours **A** and **D** are seed contours, whereas contours **B**, **C**, **E**, **F** and **G** are not. Clearly, the seed contours have the maximum elevation value but the minimum contour size in the concentric structure. The seed contours are regarded as the starting points to search outwards, and to find the next associated adjacent closed contours that enclose the seed contour. This iterative procedure continues until all seed contours and their outward closed contours are determined. It appears that a single tree has a single concentric contour pattern, while a tree cluster with two or more overlapping tree crowns has a multi-concentric contour pattern. In Fig. 1(c), **A-B-C-D-E** is a single concentric contour structure; while in Fig. 2(c), **A-B-C-E-G** and **D-F-G** together form a multi-concentric contour structure.

2.2.3.2. Construct local contour trees. After the concentric contours are identified, the topological relations among the complicated contours become more distinct, and it can be represented as a graph with a tree structure (Boyell and Ruston, 1963). The localized contour tree structure which represents the topological relationship of

concentric contours can be constructed in a prioritized manner of the elevation value. Fig. 4 shows the local contour tree structure of the concentric contour shown in Fig. 1 and Fig. 2. The local contour tree contains a root node, several internal nodes and leaf (terminal) nodes. It was constructed in a top-down manner in terms of elevation value (tree height). For the individual tree shown in Fig. 1, the local contour tree is initiated with the seed contour **A** as the leaf node, which has the highest elevation value. It is the first-level contour at the bottom of the tree. Then, the most adjacent closed contour **B** that contains the seed contour **A** was identified. Meanwhile, the local contour tree adds it as the parent node of contour **A**. This iterative process continues with a tree growing algorithm until the surrounding outermost closed contour **E** is included as the root node. The single concentric contour structure leads to a simple one-branch local contour tree (Fig. 4(a)). Similarly, for a complex overlapped trees shown in Fig. 2, the top-down searching algorithm results in a multi-branch local contour tree. As shown in Fig. 4(b), the multi-branch local contour tree is composed of a root node (**G**), four internal nodes (**B**, **C**, **E** and **F**) and two terminal nodes (**A** and **D**).

In a local contour tree, each node may have one or more child nodes, but only has one parent node. The split and merge at an internal node indicate a change of topological relationship. For example, the root node **E** in Fig. 4(a) only has one child node **D**, indicating that there is no topological relation change between them. However, the root node **G** in Fig. 4(b) has two child nodes **E** and **F**, representing a separation relationship in the sense of topological representation. For a single-branch local contour tree representing an individual tree, its topological relationship does not change from root node to the leaf node. While for a multi-branch local contour tree representing a tree cluster with crown overlap, the topological relationship

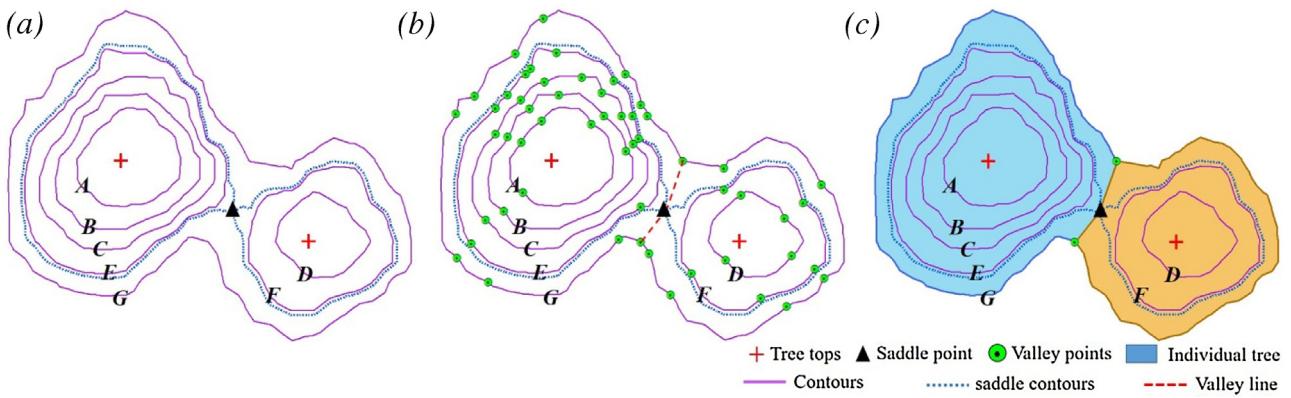


Fig. 5. Contour trees partitioning: (a) identify saddle point (black triangle) and saddle line (blue dotted line); (b) valley points extraction and valley line identification; (c) contour trees partition into two parts. (For interpretation of the references to colour in this figure legend, the reader is referred to the web version of this article.)

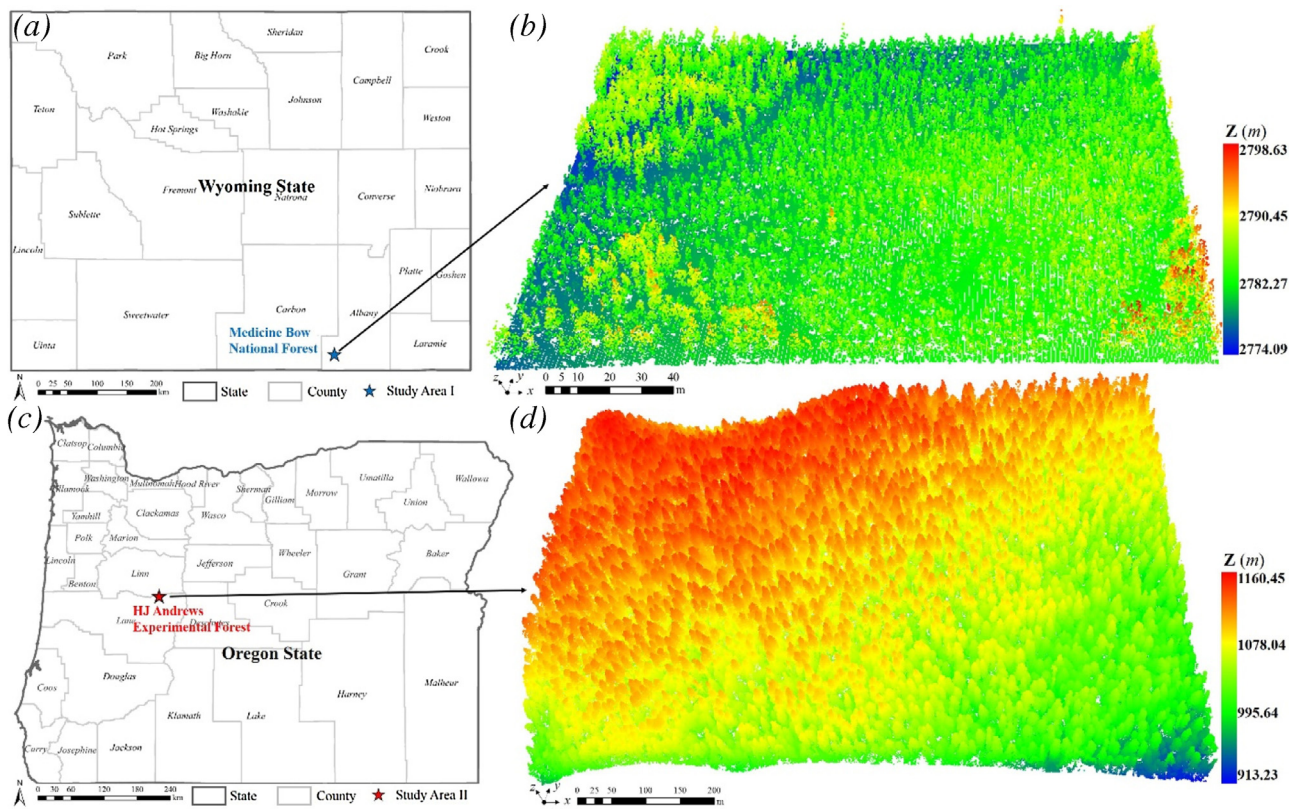


Fig. 6. Study areas: (a) location of study area I; (b) geo-referenced point cloud of study area I; (c) location of study area II; (d) geo-referenced point cloud of study area II.

changes due to the split of nodes. Clearly, the local contour tree emulates the structure of nested hierarchical relationships among forest trees. Each local contour tree represents one disjointed forest tree cluster (isolated trees or overlapped trees), and the number of local contour trees represents the total number of disjointed forest tree clusters for the entire area. The number of individual trees can be derived by counting the number of leaf nodes in each local contour tree. Obviously, the number of local contour trees approximates the number of individual trees in a sparse forest. While in a dense forest, the number of local contour trees might be far less than the number of individual trees.

2.2.4. Delineation of individual tree crowns by segmenting hierarchical crown structure

When two or more tree crowns are overlapping, the key issue for segmenting the overlapping trees into individual tree crowns is to find the segmentation points. In the smoothed CHM, the pixels representing the overlapping tree crowns are connected together (Fig. 2(a)) and the segmentation points are located in the lowest part of the overlapping areas. If we treat the overlapping trees as connected hills, the segmentation point is the lowest point on a mountain ridge between two summits. The segmentation points are called “saddle points” in the field of geomorphology. Therefore, the task of identifying segmentation points is analogous to finding saddle points on a 2D contour map.

In the 2D contour map, if two contour lines with the same elevation value touch each other, the touching point is regarded as a saddle point (black triangle in Fig. 5(a)). The contour lines touched were regarded as “saddle contours” (blue dotted lines in Fig. 5(a)) in our study. For the multi-branch local contour tree (Fig. 4(b)), the split or merge at an internal node indicates the existence of saddle points. In Fig. 4(b), the root node **G** is split into two child nodes **E** and **F**, thus the saddle point is located between node **E** and node **F**. To explicitly represent the topological structure, we simplified

the contour tree by checking if the node is a fork node. In Fig. 4(c), only the child split nodes of fork nodes are kept in the simplified contour tree. The closed contours corresponding to the nodes in the simplified contour tree are referred to as “quasi-saddle contours” (e.g., contour **G**, **E** and **F**). Apparently, the elevation difference between the quasi-saddle contour and the true saddle contour is smaller than the vertical resolution. To get accurate saddle points, the quasi-saddle contour is expanded outward within the vertical resolution to determine the saddle contour using an incremental buffering algorithm (Wu et al., 2015). The saddle contours are then used to determine the location of saddle point.

In our study, an individual tree crown is treated as a 2D spatial object whose spatial extent is defined by the outmost contour. For the single-branch local contour tree in Fig. 4(a), the boundary of the individual tree crown is the outmost closed contour corresponding to the root node **E**. While for multi-branch local contour tree, the outmost contour is the merge of two or more overlapping tree crowns. In this case, the outmost contour requires further segmentation. We need to divide the outmost contour into several objects in order that each object represents a boundary of an individual tree crown. In the above procedure, the saddle point, which is regarded as the starting point of segmentation, is derived from the contour map. The next task is to find the segmentation line which splits the outmost contour into several parts. Here we employ the valley line following method to solve this problem. Assuming the multi-concentric contours represent connected hills, the deepest continuous line within a valley is valley line. These valley lines divide the connected hills into individual hills. Similarly, the task for segmenting overlapping tree crowns is analogous to finding the valley lines passing through the saddle points. In order to extract the valley lines, we implemented the valley points and valley lines extraction method proposed by Ai (2007). The contour lines were used to construct a constrained Delaunay triangulation,

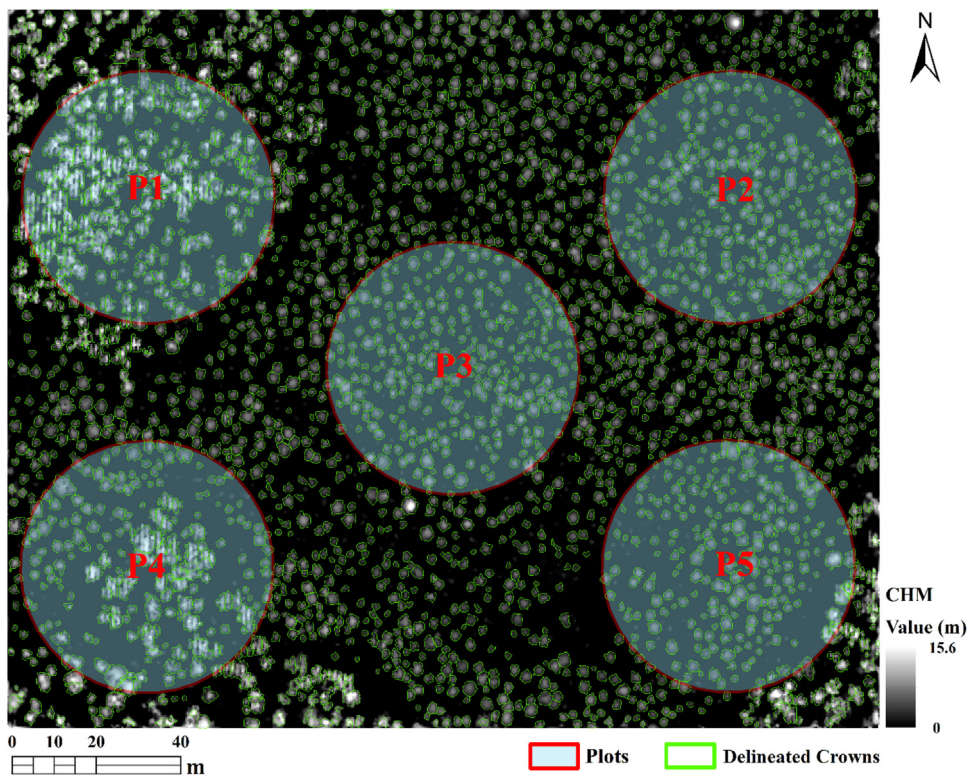


Fig. 7. Delineated tree crowns of study area I.

then a binary tree of each contour lines was constructed by using a bend segmentation method, and finally the valley point and valley lines can be detected by determining the node depth. A detailed description of the algorithm can be found in Ai (2007). In Fig. 5(b), the valley points (the green circles with black dots) were properly extracted with the method. And then the nearest valley points which are located on either side of the saddle point are identified. The valley line (red dotted line in Fig. 5(b)) passing through saddle point can be delineated by linking all the identified valley points in order. Finally, the valley line splits the outmost contour into two parts (Fig. 5(c)), and each part represents an individual tree crown.

2.2.5. Calculation of geometric and topological properties of individual trees

After the identification of individual tree crown objects, a set of morphological and geometric properties can be derived, including the tree height (h), tree crown diameter (CD), width (w), length (l), area (A), perimeter (P), and compactness index (CI). The fitted minimum bounding rectangle for each individual tree crown object is constructed. The tree width is defined as the length of the minor axis and the tree length is defined as the length of the major axis of the fitted minimum bounding rectangle. The tree height is defined as the pixel value at the location of the tree top. For the crown diameter, we take the average of the width and the length to approximate it (Wu et al., 2013). The compactness index is a widely used shape indicator (Liu et al., 2010) defined by the perimeter and area of the tree crown (Eq. (3)):

$$CI = \frac{4\pi A}{P^2} \quad (3)$$

where A and P are respectively the area and the perimeter of a tree crown object. If the shape of a tree crown object is a perfect circle, its CI is 1.0. On the contrary, when the shape is away from the circle, CI will have a smaller value than 1.0.

2.3. Accuracy assessment

Accuracy assessment for individual tree crown delineation should include evaluation of not only how many reference tree crowns in the study site are detected, but also how well the delineated individual tree crowns match the reference crowns. In our work, the accuracy assessment is evaluated by contrasting the result between the manual delineation method and the proposed automated method. Previous studies (Brandtberg et al., 2003; González-Ferreiro et al., 2013; Hu et al., 2014; Jakubowski et al., 2013; Ke et al., 2010; Li et al., 2012; Liu et al., 2015; Lu et al., 2014; Zhao et al., 2014; Zhen et al., 2015) have demonstrated that manual detection result can be used as a reference for accuracy verification. The actual positions of individual trees were determined by visual inspection of the LiDAR point cloud and aerial imagery. In most cases each individual tree could be identified by inspecting the point cloud from different angles and visual interpretation from the aerial imagery.

The accuracy was first assessed by counting omission errors (OE) and commission errors (CE). The total number of errors $TE = OE + CE$. On the basis of OE and CE , we reported detection rate $DR = (TN - OE)/TN \times 100\%$ and accuracy index (Strimbu and Strimbu, 2015) $AI = (TN - TE)/TN \times 100\%$ with the respect to the total number of individual trees (TN).

In order to investigate the matching degree between the derived tree crowns and manually delineated tree crowns, we also calculated area error ratio (AER) and area percentage (AP) for each individual tree crown. The area error ratio (AER) is defined as the ratio between the area error and the area of manual delineated crown (Eq. (4)). In Eq. (4), A_m is the area of manual delineated crown, A_d is the area of derived crown. The area percentage (AP) is defined as the ratio between the area of manual delineated crown (A_m) and the combined area of manual delineated crown and derived crown (Eq. (5)). In this manner, the AER and AP could reflect the spatial accuracy of the segmentation result. Clearly, a small AER or large

Table 1

Airborne survey parameters of two study areas.

	Study area I	Study area II
Sensor	Optech Gemini ALTM 06SEN195	Leica ALS50 Phase II laser
Scan angle	±15°	±14°
Vertical accuracy	5–35 cm (1σ)	2.1 cm (1σ)
Swath overlap	50%	≥ 50%
Range capture	Up to 4 range measurements	Up to 4 range measurements
Pulse rate	100 kHz	59 kHz
Flight altitude	600 m	Contractors discretion
Acquisition date	August 26, 2011	August 10–11, 2008

AP represent a high match degree between derived crowns and manual delineated crowns.

$$AER = \frac{A_m - A_m \cap A_d}{A_m} \quad (4)$$

$$AP = \frac{A_m}{A_m \cup A_d} \quad (5)$$

2.4. Analysis tool

The aforementioned method has been implemented as a software tool to streamline the procedures for automated individual tree extraction and morphometric properties estimation by using ArcObjects SDK for .NET and C# programming language in Microsoft Visual Studio 2010. When executing the tool, the user is asked to provide a single input, the LiDAR point clouds, and then the aforementioned procedures are executed automatically. The output data of the software tool include two feature classes: an “individual tree crowns” feature class representing the boundaries of each individual tree crown and a “tree tops” class representing the apex of each individual tree. The “individual tree crowns” feature class also records a series of attributes calculated for each individual tree, such as height, centroid, perimeter, area, volume, and some other morphometric properties. The “tree tops” feature class contains the location of apices in x and y coordinates and its height value.

3. Case studies

3.1. Study areas and LiDAR data

To test the performance of the proposed algorithm under different coniferous forest conditions, two study areas (study area I and study area II) were selected. Each study area represents a typical situation that can be encountered. Study area I and study area II have different conditions and species composition.

Study area I (Fig. 6(a)) is situated in the Medicine Bow National Forest (latitude 41°03'46"N, longitude 106°08'50"W) in the southwest of Laramie, Wyoming. Forest types at the Medicine Bow National Forest include lodgepole pine, spruce-fir, deciduous (Gambel) oak woodland, aspen, ponderosa pine, Engelmann spruce, Douglas-fir, and limber pine. Study area I is located in the center of Medicine Bow National Forest, and has a total area of 35,523 m². Ground elevation of the study area I ranges from 2774 to 2784 m above sea level. It is mainly covered with lodgepole pines. The distribution of lodgepole pines in study area I is relatively sparse. Thus, it is representative of a situation when a coniferous forest is very homogeneous with respect to species and tree sizes.

Study area II (Fig. 6(c)) is located in the HJ Andrews Experimental Forest (latitude 44°12'44"N, longitude 122°15'38"W) in the central portion of the Cascade Range of the State of Oregon, USA. Elevation of the study area ranges from 913 m above sea level to

1121 m. Study area II has a total area of 501,637 m². The dominant tree species in the rectangular study area is Douglas-fir. Study area II represents a natural coniferous forest with high-density trees characterized by low forest gaps, clustered tree crowns, and high variability in both size and height.

LiDAR data for the two study areas are available from the Open-Topography Facility (<http://www.opentopography.org/index.php>). Accessed September 2015). The LiDAR data for study area I were collected on August 26th 2011 using the Optech Gemini ALTM 06SEN195 airborne laser scanner (https://cloud.sdsc.edu/v1/AUTH_opentopography/www/metadata/NCALM/NCALM_Metadata_2011_S001_238_Biderman.pdf). Accessed May 2016). For study area II, the LiDAR data were collected during August 10th and 11th 2008 using the Leica ALS50 Phase II laser scanner (http://andrewsforest.oregonstate.edu/data/aerial/hj_andrews_report.pdf). Accessed May 2016). The LiDAR system survey parameters for these two study areas are summarized in Table 1. Study area I consists of 275,506 LiDAR points and the point density is 7.76 points/m². The LiDAR point cloud data extracted from the LAS file is in the Universal Transverse Mercator (UTM) Zone 13 N map projection and referenced to horizontal datum-NAD83 (NAD_1983.UTM_Zone_13N). Study area II consists of 6,266,321 points and the point density is 12.49 points/m². The corresponding LiDAR point cloud data extracted from the LAS file is in the UTM Zone 10 N map projection and referenced to the horizontal datum-NAD83 (NAD_1983.UTM_Zone_10N). Fig. 6(b) and (d) show the geo-referenced LiDAR point clouds of study area I and study area II.

With the progressive morphological filter, a total of 125,546 and 141,844 ground points were identified for study area I and study area II, respectively. Two raster surfaces: digital surface model (DSM) and digital elevation model (DEM) were then created from the raw LiDAR points and ground points, respectively, with a 0.25-m pixel size for each study area. The canopy height model was then created by subtracting the DEM from the DSM. After analyzing the height (relative to the DEM) histogram of the non-ground points, the minimum canopy heights d_0 were set to 0.8 m and 2.4 m for study area I and study area II, respectively. Considering vertical accuracy of the airborne LiDAR system and computational demand of the proposed algorithm, the vertical resolution d was set to 0.4 m for both study areas, which is slightly greater than the vertical accuracy (Wu et al., 2015).

3.2. Results

By using the proposed method, 2735 and 5322 individual tree crowns were detected for study area I and study area II, respectively. Fig. 7 and Fig. 8 show the results of extracted individual tree crowns overlain on the smoothed CHM for two study areas. Visual assessment of the results reveals that the proposed method successfully delineates the individual tree crowns in both two study areas.

Subsequently, the accuracy of the proposed method is evaluated. Because the manual method for reference crowns is extremely time-consuming, we only considered five selected plots in study area I and 6 plots in study area II for accuracy assessment. As shown in Fig. 7 and Fig. 8, a set of 5 circular plots (P1, P2, P3, P4 and P5) with a 30-m radius and six circular plots (P6, P7, P8, P9, P10 and P11) with a 100-m radius were laid out within each study area. All 11 circular plots were distributed uniformly in each study area. Then, the 11 plots were used for the subsequent accuracy assessment.

The accuracy of the proposed algorithm for the 11 selected plots are shown in Table 2 and Table 3. The proposed method obtained an average detection rate DR of 96.11% and an average accuracy index AI of 94.21% for study area I, and an average detection rate

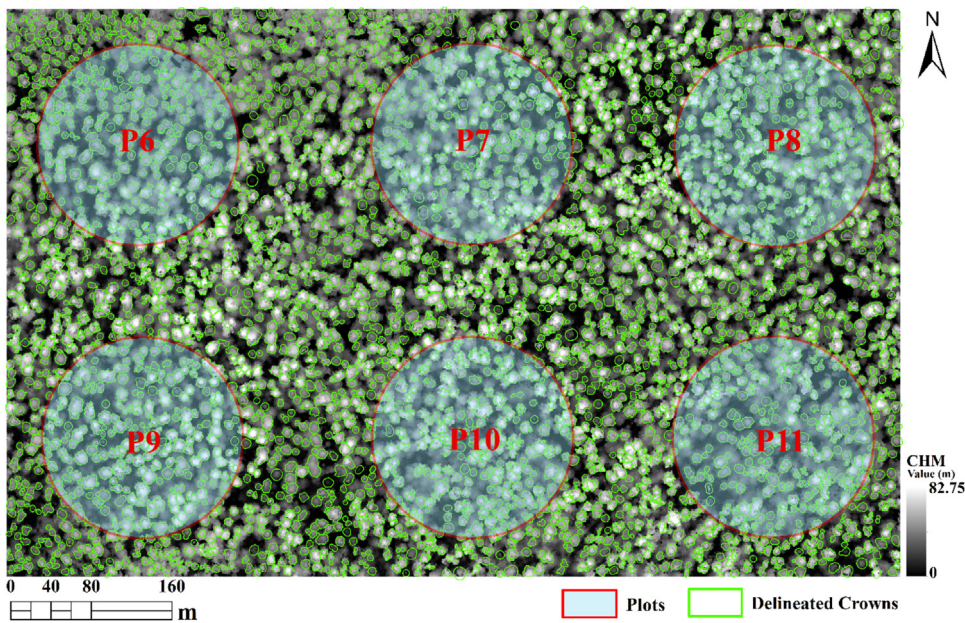


Fig. 8. Delineated tree crowns of study area II.

Table 2
Detection accuracy for study area I.

Plots	TN	OE	CE	DR (%)	AI (%)
P1	212	8	13	96.23	90.09
P2	264	11	0	95.83	95.83
P3	284	5	0	98.24	98.24
P4	191	10	5	94.76	92.15
P5	246	11	2	95.53	94.72
Average	--	--	--	96.11	94.21

Table 3
Detection accuracy for study area II.

Plots	TN	OE	CE	DR (%)	AI (%)
P6	225	19	37	91.56	75.11
P7	194	15	36	92.27	73.71
P8	221	22	31	90.04	76.02
P9	210	7	32	96.67	81.43
P10	188	11	38	94.15	73.94
P11	198	18	41	90.91	70.20
Average	--	--	--	92.60	75.07

DR of 92.60% and an average accuracy index AI of 75.07% for study area II. For the five plots (P1, P2, P3, P4 and P5) in study area I, P3 has the largest DR (98.24%) and AI (98.24%). In study area II, plot 9 (P9) has the largest DR (96.67%) and AI (81.43%). It is evident that the localized contour tree method has a high detection rate and relatively high accuracy in both study areas. From Table 2, it is clearly observed that the omission error is much larger than the commission error in study area I. In contrast to study area I, the commission error is much worse in study area II. Because of high dense trees and noise errors in CHM, over-segmentation problem appears more serious in study area II. Apart from calculation of detection accuracy for every single plot, the area accuracy values for all plots respectively represented by AER and AP were calculated. The AER ranges from 0.01% to 50.58% with a standard deviation of 7.07% in study area I. For the study area II, the AER ranges from 0.62% to 69.65% with an average of 36.01%. For both areas, the average AP is greater than 83%. This indicates that the delineated tree crowns are well matched with the reference crowns. Therefore, the proposed method can achieve relatively high accuracy for both sparse and dense coniferous forests.

Table 4
Detection accuracy comparison of three selected methods.

Study areas and plots	LMF-AI (%)	WS-AI (%)	Proposed-AI (%)
Study area I	P1	87.26	83.02
	P2	93.56	90.91
	P3	92.96	97.18
	P4	88.48	85.34
	P5	88.62	88.62
	Average	90.18	89.01
Study area II	P6	69.33	73.33
	P7	71.65	74.22
	P8	69.23	75.11
	P9	72.86	78.57
	P10	68.09	72.87
	P11	64.65	68.69
Average		69.30	73.80
			75.07

4. Discussion

4.1. Comparison with previous studies

In this part, we implemented two existing popular methods: the local maxima filter (LMF) method (Hyppä et al., 2001) and the watershed segmentation (WS) method (Chen et al., 2006) for comparison. Table 4 shows the results comparison of AI. For the five selected plots in study area I, the LMF method was able to identify tree crowns with an average accuracy of 90.18%, whereas the WS method produced an average accuracy of 89.01%. The LMF method performs slightly better than the WS method. This is probably due to the serious over-segmentation problem of the WS method. The WS method is hampered by its inability to delineate tree crowns under sparse forest conditions (Gleason and Im, 2012), which leads to the lowest accuracy for study area I. Our proposed method performs the best with its accuracy 4.62% higher than the other two methods. In study area II, a denser forest condition, the overall accuracy of our method ranges from 70.2% to 81.43%, with an average delineation accuracy of 75.07%. This resulting accuracy is slightly higher than the WS method, and 5.7% higher than the LMF method.

A major cause of the difference in accuracy between the two previous methods and our proposed method lies within those crowns that are over-segmented. We found that all three methods produced very similar omission errors but with considerably

different commission errors. All methods failed to segment certain tree crowns correctly, yet the magnitude of the commission errors for such crowns in the LMF method and the WS method is much more pronounced than that in our proposed method. In forest conditions such as the study area II, where many trees crowns are heavily overlapped and densely located with no canopy gaps exist, the LMF and WS methods produced 3%–6% higher over-segmented tree crowns than the proposed method. This may be explained by the fact that the LMF and WS methods are based on the elevation value of the pixels in the smoothed CHM, while the proposed method is based on contour lines formed by interpolation. The set of contour lines interpolated from the smoothed CHM is a higher-level representation of CHM, which reduces some spurious noises to some extent.

Previous studies (Chen et al., 2006; Gleason and Im, 2012; González-Ferreiro et al., 2013; Kwak et al., 2007; Persson et al., 2002) have reported that it is possible to detect between 40% and 74% of trees in different forests. We identified Persson et al. (2002), Gleason and Im (2012), Strîmbu and Strîmbu (2015) and Liu et al. (2015) as somewhat appropriate studies for comparison with our study areas due to similar forest conditions and LiDAR dataset. Strîmbu and Strîmbu (2015) detected the individual trees with an AI between 91.4% and 98.7% when applying their method to an ‘easy’ test site similar to our study area I. For a dense forest condition, Persson et al. (2002) reported that 71% of the trees were correctly detected in their test forest; Gleason and Im (2012) reported that their method was able to identify tree crowns with 72.5% classification accuracy; Strîmbu and Strîmbu (2015) reported that the best AI for a ‘hard’ test site is 74.75%; and Liu et al. (2015) shown that their proposed method achieved 74% and 78% as overall accuracy for two test sites. These studies indicate previous methods have reached a very high precision. Nevertheless, our method performed as well as or better than the previous methods by 1–4% improvement in terms of AI. Although this might not be considered as a significant increase in overall accuracy over existing methods, more accurate results were obtained by our proposed method in local areas (such as P1–P5), especially in sparse forests. In P1 to P5, our proposed method performs the best with its average accuracy 4.03% higher than the LMF method and 5.2% higher than the WS method. Furthermore, the number of the delineated crowns was equal to the number of markers and local maxima used when applying the LMF method and the WS method. Therefore, the selected markers or local maxima, which are very difficult to determine, act as one of the important factors to affect the delineation result. Our algorithm used prior knowledge about the spatial relationships based on hierarchical structure of tree crowns to determine the number of the delineated crowns, this means that a more detailed and profound forest structure can be acquired by utilizing our method once the trees are segmented out.

Table 5
Crown area accuracy comparison of three selected methods.

Study area	Statistics	LMF		WS		Proposed	
		AER (%)	AP (%)	AER (%)	AP (%)	AER (%)	AP (%)
I	Max	52.39	97.25	50.39	91.71	50.58	99.22
	Min	1.99	68.23	0.14	62.28	0.01	50.36
	Average	12.40	88.32	6.44	85.52	7.61	87.80
	StdDev	7.79	6.13	9.88	6.29	7.07	8.00
II	Max	83.96	99.90	89.67	99.65	69.65	99.99
	Min	0.17	29.32	0.10	28.50	0.62	30.35
	Average	37.96	83.26	37.36	83.04	36.01	83.43
	StdDev	23.34	12.04	22.83	12.42	17.90	12.43

Besides AI, the delineated boundaries of individual tree crowns vary for different methods. To evaluate the tree crown area accuracy of the three methods, the delineation results of all 11 plots (P1–P11) are selected for comparison. The statistics for the comparison results are summarized in Table 5. The average AER of the LMF method, the WS method and the proposed method in study area II is 37.96%, 37.36% and 36.01%, respectively. And the average AP of these three methods in study area II is 83.26%, 83.04% and 83.43%, respectively. It is clear that the proposed method has comparable performance compared to the LMF method and the WS method. Among the 11 groups of delineation results, we selected a sparse plot (P3) and a dense plot (P9) from the two study areas to perform a visual evaluation. Fig. 9 shows that there are slight differences in the shape boundary between the derived tree crowns and the reference crowns. From Fig. 9, we found that tree crown boundaries delineated by the localized contour tree method are much smoother than the results extracted by the LMF method and WS method. The LMF and WS method are pixel-based analysis approaches, so the boundaries delineated from the CHM appear to be jagged. In our proposed method, the contour lines are interpolated from the CHM, which improves the appearance of jagged or over-sharpened edges. From Fig. 9(c) and (f), we also noticed that most tree crown shapes delineated by the proposed method are smaller than the reference tree crown shapes. This is partly due to the fact that only closed contour lines were considered in the proposed method. In fact, some contour lines with low height value might not be closed when derived from the CHM corresponding to the dense forest. Due to the topological vagueness, tree crown information carried by these open contour lines are lost. Nevertheless, the standard deviation of the AER and AP for the three methods are very close. Therefore, the proposed approach owns comparable reliability compared with the LMF method and WS method.

For individual tree delineation, there are two important factors affecting the accuracy: the delineation algorithm used and the canopy structure (Kaarinen et al., 2012; Vauhkonen et al., 2012). Individual tree delineation, especially in heterogeneous conditions,

Table 6
Impact of vertical resolution d on delineation accuracy of individual tree crowns in study area I.

d (m)	P1		P2		P3		P4		P5	
	DR (%)	AI(%)	DR (%)	AI(%)	DR(%)	AI(%)	DR (%)	AI(%)	DR(%)	AI(%)
0.1	100.00	84.43	100.00	95.45	99.65	95.07	100.00	85.34	99.59	93.09
0.2	100.00	85.85	100.00	95.83	98.94	97.18	100.00	89.53	98.78	92.68
0.3	98.58	88.21	98.11	96.21	98.59	98.24	96.86	90.05	97.15	94.31
0.4	96.23	90.09	95.83	95.83	98.24	98.24	94.76	92.15	95.53	94.72
0.5	95.75	90.09	94.70	94.70	96.83	96.48	94.76	92.15	95.53	94.72
0.6	94.81	90.57	94.32	94.32	95.42	95.07	93.72	91.62	95.12	94.72
0.7	93.40	89.15	92.80	92.80	95.42	95.42	92.15	90.05	94.31	94.31
0.8	91.98	88.68	92.80	92.80	94.37	94.37	91.62	90.58	93.50	93.50
0.9	88.68	86.79	92.05	92.05	92.96	92.96	90.58	90.58	92.28	92.28
1.0	84.91	84.91	90.53	90.53	90.85	90.85	89.01	89.01	91.87	91.87
Average	94.43	87.88	95.11	94.05	96.13	95.39	94.35	90.10	95.37	93.62
StdDev	4.89	2.25	3.32	1.92	2.86	2.32	3.74	1.98	2.57	1.08

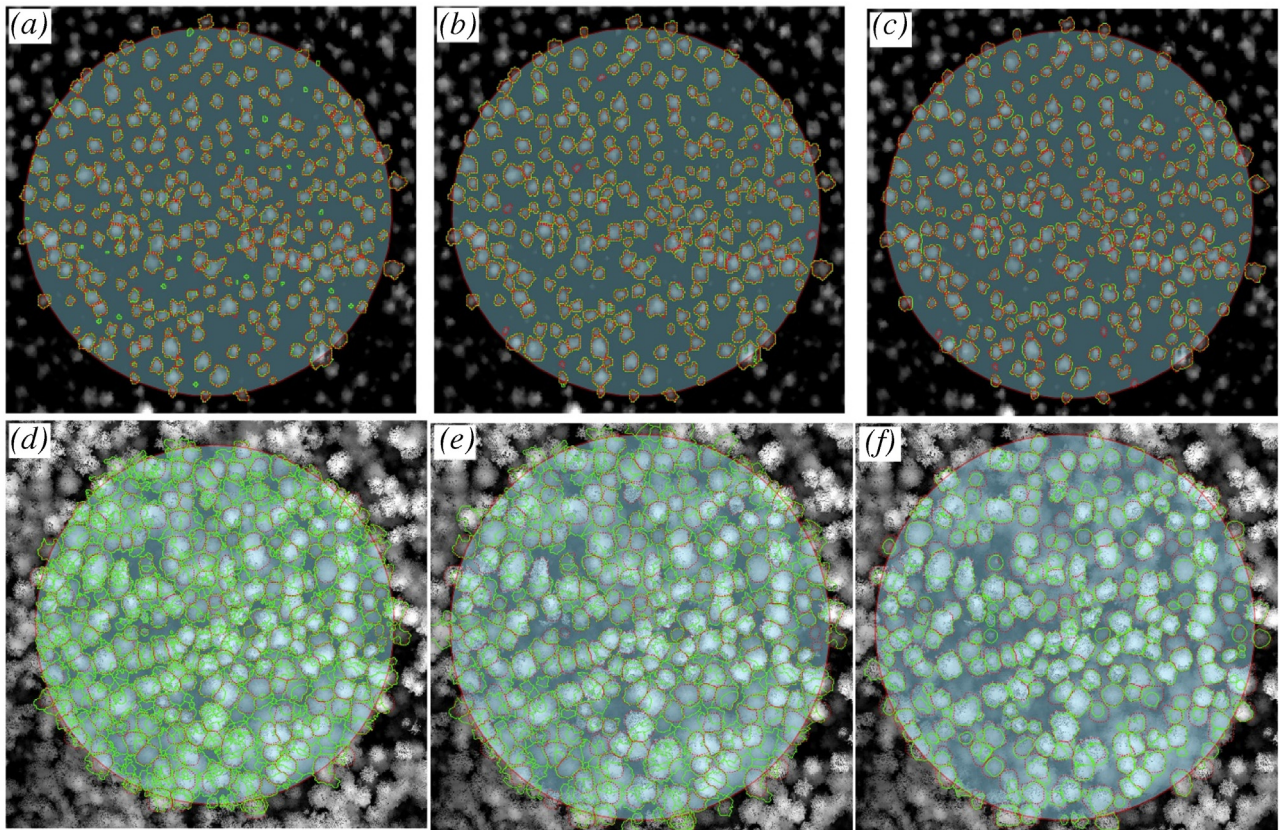


Fig. 9. Delineated tree crowns comparison: (a) the local maxima filter result of P3; (b) the watershed segmentation result of P3; (c) the localized contour tree detection result of P3; (d) the local maxima filter result of P9; (e) the watershed segmentation result of P9; (f) the localized contour tree detection result of P9. Delineated tree crowns are solid green lines and reference tree crowns are dotted red lines in all figures. (For interpretation of the references to colour in this figure legend, the reader is referred to the web version of this article.).

tends to over-detect the number of individual trees because of the wider and irregular canopy shapes. In the present study, we used the localized contour tree approach to identify the canopy structure. We describe a hierarchical data structure that captures and organizes the canopy structure and provides support for delineation of individual tree crowns. The approach is based on the geometrical properties of the tree canopies and their topological relationships with neighbors. While the approach can reduce the commission errors to some extent, it is still influenced by the complex canopy structure. Our method has difficulty extracting multi-canopy trees since they can have several local maxima points. The multiple canopies of an individual tree will form a multi-concentric contour structure, and it could eventually be detected as several individual trees.

4.2. Sensitivity analysis of d

There is only one parameter, the vertical resolution d , needs to be set in our study. It should be noted that the contour internal is the intrinsic limitation of contouring, which is the major factor that affects commission or omission errors. Selection of a small d will help to detect small trees, but it might result in high computation and large commission errors. A large d will help to enhance computing efficiency, but it might lead to large omission errors. In general, the selection of d varies based on the input airborne LiDAR point clouds. It might be difficult to automatically adjust the threshold d for different airborne LiDAR point clouds without prior knowledge. In our study, a range of d (from 0.1 to 1 m) for contour generation in all the 11 Plots (P1 to P11) were conducted to evaluate its impact on delineation accuracy of individual tree crowns,

and the results are shown in Table 6 and Table 7. When d changes from 0.1 to 1 m, we found that the DR decreased gradually while the AI increased at first, then decreased. The results indicate that the omission error increases while the commission error decreases when d changes from 0.1 to 1 m. When d is very small, many little local maxima could be counted by the contouring, which results in tree crowns being over-segmented. When d is very large, many small trees will be missed from the contour lines, leading to the under-segmentation issues. In general, a small d will lead to large commission error whereas a large d will lead to large omission error. Besides, it is clear that the AI is relatively high when d changes from 0.3 to 0.5 m and 0.4–0.9 m for study area I and study area II, respectively. From Fig. 7 and Fig. 8, the maximum tree height for study area I and study area II are 15.6 m and 82.75 m, respectively. So the AI is very sensitive and unstable for study area I with lower trees when d changes from 0.1 m to 1 m. For study area II with higher trees, the AI is relatively stable when d changes from 0.4 to 0.9 m. These results suggest that a smaller d can be used for lower trees and a larger d is recommended to use for higher trees.

5. Conclusion

Investigation and analysis of forest resources at individual tree level play an important role in forest growth modeling, forest monitoring, and forest inventory. High-resolution LiDAR technologies provide an extraordinary capability for acquiring detailed information of vegetation in a forest, which makes it possible to detect canopy structures and quantify individual trees. In this research, we presented an automated segmentation method for individual trees extraction using airborne LiDAR data. We adopted and refined

Table 7Impact of vertical resolution d on delineation accuracy of individual tree crowns in study area II.

d (m)	P6		P7		P8		P9		P10		P11	
	DR(%)	AI(%)										
0.1	100.00	58.22	100.00	59.79	100.00	55.66	100.00	49.05	100.00	57.98	100.00	53.54
0.2	99.11	71.56	100.00	63.40	99.10	62.44	100.00	59.52	97.87	67.02	100.00	56.57
0.3	96.00	72.44	96.39	70.10	94.57	72.40	99.05	76.67	95.21	72.34	96.46	67.68
0.4	91.56	75.11	92.27	73.71	90.05	76.02	96.67	81.43	94.15	73.94	90.91	70.20
0.5	90.22	75.56	91.24	73.20	87.33	73.76	94.29	80.48	86.17	67.55	89.90	69.19
0.6	90.22	75.11	89.18	72.68	87.33	75.11	93.33	79.52	84.04	66.49	85.86	67.68
0.7	89.33	74.22	84.54	68.04	83.71	73.76	89.52	79.05	81.38	67.02	81.31	68.69
0.8	87.11	73.33	82.99	68.04	81.90	73.30	87.62	79.52	79.26	67.02	76.26	65.66
0.9	84.44	72.00	76.80	66.49	78.73	71.49	86.19	79.05	76.06	67.55	75.25	65.15
1.0	79.11	68.44	73.71	64.95	75.11	69.68	83.33	76.67	70.74	62.77	72.22	63.64
Average	90.71	71.60	88.71	68.04	87.78	70.36	93.00	74.10	86.49	66.97	86.82	64.80
StdDev	6.45	5.16	9.13	4.55	8.32	6.42	6.06	10.83	9.93	4.43	10.31	5.55

the localized contour tree algorithm and made it applicable for individual tree crown delineation. The proposed approach captures topological structure of tree crowns and quantifies their topological relationships by using the graph theory-based localized contour tree method, and finally segments individual tree crowns by analogy of recognizing hills from a topographic map. The automated procedure for individual tree crown delineation described in our case studies demonstrates its stability and reliability.

The primary contributions of the proposed method are three-fold. First, we applied the localized contour tree method to represent the hierarchical structures of tree crowns. The complex structure of tree crowns can be easily simplified and represented using a graph. Second, we adopted the valley line following method to partition the hierarchical structures and separate individual tree crowns. The topographic information helps us to identify segmentation points for extracting individual tree crowns from overlapping tree crowns. The hierarchical structures, which are regarded as connected mountains, are used for extraction of topographic feature points. By determining the valley line passing through the saddle point and its related valley points, the hierarchical structures are naturally partitioned into different parts. Third, compared with previous methods in the literature, the required input parameters of our method is fewer. There is only one parameter needs to be specified, which makes our method more convenient and readily operational.

This study demonstrated that our proposed method is very promising and the experimental results are encouraging, especially considering the optimal parameters used in accuracy assessment. Compared with the watershed segmentation and the local maxima filter method, the proposed method improves the detection accuracy by 1.8%–4.5% and reduces the commission errors by 3%–6%. The constructed local contour trees and the delineated tree crowns can be further used for computing various geometric properties and tree parameters. The properties derived from our method provide comprehensive and essential information for various forest applications. By using graph theory, we construct an abstract representation of the topological relationships of tree crowns and canopy structure. Besides, the hierarchical contours structures derived in our study have the potential to model 3D single trees.

There are still some limitations with our method. In a highly heterogeneous forest with various canopy layers, small trees could be covered by big trees and are therefore not visible in the CHM. In this case, our method might not deliver good results. Besides, our method is tested only in coniferous forests. In future research, we will test and improve the method under various forest conditions and make further improvements in the algorithms. In addition, we will combine topological information derived from the proposed method and spectral information obtained from airborne LiDAR intensity/full-waveform data to improve the segmentation pro-

cess. This process could be beneficial to the partitioning of different species and age classes.

Acknowledgments

This work was supported in part by the National Natural Science Foundation of China under Grant 41471449, in part by the Natural Science Foundation of Shanghai under Grant 14ZR1412200, and in part by the Fundamental Research Funds for the Central Universities of China. Bin Wu is sponsored by the China Scholarship Council under the State Scholarship Fund (No.201506140090) to study abroad.

References

- Ai, T., 2007. The drainage network extraction from contour lines for contour line generalization. *ISPRS J. Photogramm. Remote Sens.* 62, 93–103.
- Boyell, R.L., Ruston, H., 1963. Hybrid techniques for real-time radar simulation. In: *Proceedings of the Fall Joint Computer Conference IEEE*, Las Vegas, Nevada, pp. 445–458.
- Brandtberg, T., Warner, T.A., Landenberger, R.E., McGraw, J.B., 2003. Detection and analysis of individual leaf-off tree crowns in small footprint: high sampling density lidar data from the eastern deciduous forest in North America. *Remote Sens. Environ.* 85, 290–303.
- Chang, A., Eo, Y., Kim, Y., Kim, Y., 2012. Identification of individual tree crowns from LiDAR data using a circle fitting algorithm with local maxima and minima filtering. *Remote Sens. Lett.* 4, 29–37.
- Chen, Q., Baldocchi, D., Gong, P., Kelly, M., 2006. Isolating individual trees in a savanna woodland using small footprint lidar data. *Photogramm. Eng. Remote Sens.* 72, 923–932.
- Ene, L., Næsset, E., Gobakken, T., 2012. Single tree detection in heterogeneous boreal forests using airborne laser scanning and area-based stem number estimates. *Int. J. Remote Sens.* 33, 5171–5193.
- Estornell, J., Velázquez-Martí, B., López-Cortés, I., Salazar, D., Fernández-Sarría, A., 2014. Estimation of wood volume and height of olive tree plantations using airborne discrete-return LiDAR data. *GISci Remote Sens.* 51, 17–29.
- Gleason, C.J., Im, J., 2012. A fusion approach for tree crown delineation from LiDAR data. *Photogramm. Eng. Remote Sens.* 78, 679–692.
- González-Ferreiro, E., Diéguez-Aranda, U., Miranda, D., 2012. Estimation of stand variables in *Pinus radiata* D: Don plantations using different LiDAR pulse densities. *Forestry* 85, 281–292.
- González-Ferreiro, E., Diéguez-Aranda, U., Barreiro-Fernández, L., Buján, S., Barbosa, M., Suárez, J.C., Bye, I.J., Miranda, D., 2013. A mixed pixel- and region-based approach for using airborne laser scanning data for individual tree crown delineation in *Pinus radiata* D. Don plantations. *Int. J. Remote Sens.* 34, 7671–7690.
- Hollaas, M., Wagner, W., Maier, B., Schadauer, K., 2007. Airborne laser scanning of forest stem volume in a mountainous environment. *Sensors* 7, 1559–1577.
- Holmgren, J., Nilsson, M., Olsson, H., 2003. Estimation of tree height and stem volume on plots using airborne laser scanning. *For. Sci.* 49, 419–428.
- Hu, B., Li, J., Jing, L., Judah, A., 2014. Improving the efficiency and accuracy of individual tree crown delineation from high-density LiDAR data. *Int. J. Appl. Earth Obs. Geoinf.* 26, 145–155.
- Huang, Y., Chen, Z., Wu, B., Chen, L., Mao, W., Zhao, F., Wu, J., Wu, J., Yu, B., 2015. Estimating roof solar energy potential in the downtown area using a GPU-Accelerated solar radiation model and airborne LiDAR data. *Remote Sens.* 7, 17212–17233.
- Hyppä, J., Kelle, O., Leikonen, M., Inkkinen, M., 2001. A segmentation-based method to retrieve stem volume estimates from 3-D tree height models produced by laser scanners. *IEEE Trans. Geosci. Remote Sens.* 39, 969–975.

- Hyyppä, J., Hyyppä, H., Leckie, D., Gougeon, F., Yu, X., Maltamo, M., 2008. Review of methods of small-footprint airborne laser scanning for extracting forest inventory data in boreal forests. *Int. J. Remote Sens.* 29, 1339–1366.
- Hyyppä, J., Yu, X., Hyyppä, H., Vastaranta, M., Holopainen, M., Kukko, A., Kaartinen, H., Jaakkola, A., Vaaja, M., Koskinen, J., 2012. Advances in forest inventory using airborne laser scanning. *Remote Sens.* 4, 1190–1207.
- Jakubowski, M.K., Li, W., Guo, Q., Kelly, M., 2013. Delineating individual trees from Lidar data: a comparison of vector-and raster-based segmentation approaches. *Remote Sens.* 5, 4163–4186.
- Kaartinen, H., Hyyppä, J., Yu, X., Vastaranta, M., Hyyppä, H., Kukko, A., Holopainen, M., Heipke, C., Hirschmugl, M., Morsdorf, F., 2012. An international comparison of individual tree detection and extraction using airborne laser scanning. *Remote Sens.* 4, 950–974.
- Ke, Y., Zhang, W., Quackenbush, L.J., 2010. Active contour and hill climbing for tree crown detection and delineation. *Photogramm. Eng. Remote Sens.* 76, 1169–1181.
- Koch, B., Heyder, U., Weinacker, H., 2006. Detection of individual tree crowns in airborne lidar data. *Photogramm. Eng. Remote Sens.* 72, 357–363.
- Kwak, D.-A., Lee, W.-K., Lee, J.-H., Biging, G., Gong, P., 2007. Detection of individual trees and estimation of tree height using LiDAR data. *J. For. Res.* 12, 425–434.
- Larsen, M., Eriksson, M., Descombes, X., Perrin, G., Brandtberg, T., Gougeon, F.A., 2011. Comparison of six individual tree crown detection algorithms evaluated under varying forest conditions. *Int. J. Remote Sens.* 32, 5827–5852.
- Lee, H., Slatton, K.C., Roth, B.E., Cropper, W.P., 2010. Adaptive clustering of airborne LiDAR data to segment individual tree crowns in managed pine forests. *Int. J. Remote Sens.* 31, 117–139.
- Li, W., Guo, Q., Jakubowski, M.K., Kelly, M., 2012. A new method for segmenting individual trees from the lidar point cloud. *Photogramm. Eng. Remote Sens.* 78, 75–84.
- Lichstein, J.W., Dushoff, J., Ogle, K., Chen, A., Purves, D.W., Caspersen, J.P., Pacala, S.W., 2010. Unlocking the forest inventory data: relating individual tree performance to unmeasured environmental factors. *Ecol. Appl.* 20, 684–699.
- Lin, C., Thomson, G., Lo, C.-S., Yang, M.-S., 2011. A multi-level morphological active contour algorithm for delineating tree crowns in mountainous forest. *Photogramm. Eng. Remote Sens.* 77, 241–249.
- Liu, H., Wang, L., Sherman, D., Gao, Y., Wu, Q., 2010. An object-based conceptual framework and computational method for representing and analyzing coastal morphological changes. *Int. J. Geogr. Inf. Sci.* 24, 1015–1041.
- Liu, T., Im, J., Quackenbush, L.J., 2015. A novel transferable individual tree crown delineation model based on Fishing Net Dragging and boundary classification. *ISPRS J. Photogramm. Remote Sens.* 110, 34–47.
- Lu, X., Guo, Q., Li, W., Flanagan, J., 2014. A bottom-up approach to segment individual deciduous trees using leaf-off lidar point cloud data. *ISPRS J. Photogramm. Remote Sens.* 94, 1–12.
- Means, J.E., Acker, S.A., Harding, D.J., Blair, J.B., Lefsky, M.A., Cohen, W.B., Harmon, M.E., McKee, W.A., 1999. Use of large-Footprint scanning airborne lidar to estimate forest stand characteristics in the western cascades of oregon. *Remote Sens. Environ.* 67, 298–308.
- Means, J.E., Acker, S.A., Fitt, B.J., Renslow, M., Emerson, L., Hendrix, C.J., 2000. Predicting forest stand characteristics with airborne scanning lidar. *Photogramm. Eng. Remote Sens.* 66, 1367–1372.
- Morsdorf, F., Meier, E., Kötz, B., Itten, K.I., Dobbertin, M., Allgöwer, B., 2004. LiDAR-based geometric reconstruction of boreal type forest stands at single tree level for forest and wildland fire management. *Remote Sens. Environ.* 92, 353–362.
- Persson, A., Holmgren, J., Söderman, U., 2002. Detecting and measuring individual trees using an airborne laser scanner. *Photogramm. Eng. Remote Sens.* 68, 925–932.
- Pirotti, F., 2010. Assessing a template matching approach for tree height and position extraction from lidar-Derived canopy height models of *pinus pinaster* stands. *Forests* 1, 194–208.
- Popescu, S.C., Wynne, R.H., 2004. Seeing the trees in the forest. *Photogramm. Eng. Remote Sens.* 70, 589–604.
- Popescu, S.C., Wynne, R.H., Nelson, R.F., 2003. Measuring individual tree crown diameter with lidar and assessing its influence on estimating forest volume and biomass. *Can. J. Remote Sens.* 29, 564–577.
- Reitberger, J., Krzystek, P., Stilla, U., 2008. Analysis of full waveform LiDAR data for the classification of deciduous and coniferous trees. *Int. J. Remote Sens.* 29, 1407–1431.
- Reitberger, J., Schnorr, C., Krzystek, P., Stilla, U., 2009. 3D segmentation of single trees exploiting full waveform LiDAR data. *ISPRS J. Photogramm. Remote Sens.* 64, 561–574.
- Strímbu, V.F., Strímbu, B.M., 2015. A graph-based segmentation algorithm for tree crown extraction using airborne LiDAR data. *ISPRS J. Photogramm. Remote Sens.* 104, 30–43.
- Unger, D.R., Hung, I.K., Brooks, R., Williams, H., 2014. Estimating number of trees, tree height and crown width using Lidar data. *GISci. Remote Sens.* 51, 227–238.
- Vauhkonen, J., Ene, L., Gupta, S., Heinzel, J., Holmgren, J., Pitkänen, J., Solberg, S., Wang, Y., Weinacker, H., Hauglin, K.M., Lien, V., Packalén, P., Gobakken, T., Koch, B., Næsset, E., Tokola, T., Maltamo, M., 2012. Comparative testing of single-tree detection algorithms under different types of forest. *Forestry* 85, 27–40.
- Vega, C., Hamrouni, A., El Mokhtari, S., Morel, J., Bock, J., Renaud, J.P., Bouvier, M., Durrieu, S., 2014. PTrees: a point-based approach to forest tree extraction from lidar data. *Int. J. Appl. Earth Obs. Geoinf.* 33, 98–108.
- Wagner, W., Hollaus, M., Briese, C., Ducic, V., 2008. 3D vegetation mapping using small-footprint full-waveform airborne laser scanners. *Int. J. Remote Sens.* 29, 1433–1452.
- Wang, Y., Weinacker, H., Koch, B., 2008. A lidar point cloud based procedure for vertical canopy structure analysis and 3D single tree modelling in forest. *Sensors* 8, 3938–3951.
- Wu, B., Yu, B., Yue, W., Shu, S., Tan, W., Hu, C., Huang, Y., Wu, J., Liu, H., 2013. A voxel-based method for automated identification and morphological parameters estimation of individual street trees from mobile laser scanning data. *Remote Sens.* 5, 584–611.
- Wu, Q., Liu, H., Wang, S., Yu, B., Beck, R., Hinkel, K., 2015. A localized contour tree method for deriving geometric and topological properties of complex surface depressions based on high-resolution topographical data. *Int. J. Geogr. Inf. Sci.* 29, 2041–2060.
- Wu, B., Yu, B., Huang, C., Wu, Q., Wu, J., 2016. Automated extraction of ground surface along urban roads from mobile laser scanning point clouds. *Remote Sens. Lett.* 7, 170–179.
- Yu, B., Liu, H., Wu, J., Hu, Y., Zhang, L., 2010a. Automated derivation of urban building density information using airborne LiDAR data and object-based method. *Landsc. Urban Plan.* 98, 210–219.
- Yu, X., Hyyppä, J., Holopainen, M., Väistäraanta, M., 2010b. Comparison of area-Based and individual tree-Based methods for predicting plot-Level forest attributes. *Remote Sens.* 2, 1481–1495.
- Yu, X., Hyyppä, J., Väistäraanta, M., Holopainen, M., Viitala, R., 2011. Predicting individual tree attributes from airborne laser point clouds based on the random forests technique. *ISPRS J. Photogramm. Remote Sens.* 66, 28–37.
- Yu, S., Yu, B., Song, W., Wu, B., Zhou, J., Huang, Y., Wu, J., Zhao, F., Mao, W., 2016. View-based greenery: a three-dimensional assessment of city buildings' green visibility using Floor Green View Index. *Landsc. Urban Plan.* 152, 13–26.
- Zhang, K., Chen, S.-C., Whitman, D., Shyu, M.-L., Yan, J., Zhang, C., 2003. A progressive morphological filter for removing nonground measurements from airborne LiDAR data. *IEEE Trans. Geosci. Remote Sens.* 41, 872–882.
- Zhang, C., Zhou, Y., Qiu, F., 2015. Individual tree segmentation from LiDAR point clouds for urban forest inventory. *Remote Sens.* 7, 7892–7913.
- Zhao, D., Pang, Y., Li, Z., Liu, L., 2014. Isolating individual trees in a closed coniferous forest using small footprint lidar data. *Int. J. Remote Sens.* 35, 7199–7218.
- Zhen, Z., Quackenbush, L.J., Stehman, S.V., Zhang, L., 2015. Agent-based region growing for individual tree crown delineation from airborne laser scanning (ALS) data. *Int. J. Remote Sens.* 36, 1965–1993.